Influence of Displacement Amplitude and Vertical Load on the Horizontal Dynamic and Static Behavior of Helical Wire Rope Isolators

Nicolò Vaiana, Mariacristina Spizzuoco, Giorgio Serino

Abstract—In this paper, the results of experimental tests performed on a Helical Wire Rope Isolator (HWRI) are presented in order to describe the dynamic and static behavior of the selected metal device in three different displacements ranges, namely small, relatively large, and large displacements ranges, without and under the effect of a vertical load. A testing machine, allowing to apply horizontal displacement or load histories to the tested bearing with a constant vertical load, has been adopted to perform the dynamic and static tests. According to the experimental results, the dynamic behavior of the tested device depends on the applied displacement amplitude. Indeed, the HWRI displays a softening and a hardening stiffness at small and relatively large displacements, respectively, and a stronger nonlinear stiffening behavior at large displacements. Furthermore, the experimental tests reveal that the application of a vertical load allows to have a more flexible device with higher damping properties and that the applied vertical load affects much less the dynamic response of the metal device at large displacements. Finally, a decrease in the static to dynamic effective stiffness ratio with increasing displacement amplitude has been observed.

Keywords—Base isolation, earthquake engineering, experimental hysteresis loops, wire rope isolators.

I. INTRODUCTION

WIRE rope isolators are metal devices that have demonstrated to be effective in protecting sensitive equipment from shock and vibration [1] and are currently adopted as seismic devices for the protection of equipment in buildings [2] and for the reduction of seismic demand of high voltage ceramic circuit breakers [3]-[6]. They have been also used as vertical isolation devices in the new antiseismic basements for earthquake protection of the two statues known as "Bronzes of Riace" [7].

Wire rope isolators are made of a stainless steel cable and two aluminum alloy or steel retainer bars where the cable is embedded. These metal devices are deformable in both vertical and horizontal directions and possess a significant dissipation capacity due to the interior rubbing and sliding friction between the individual strand wires and between the intertwined strands [1]. Dynamic and static behavior of wire rope isolators depend on their geometrical characteristics, such as the height to width ratio, the diameter of the wire rope, the number of strands, the cable length, the cable twist, the number of cables per section, and the number of loops [2].

A HWRI, manufactured by Powerflex s.r.l (Limatola, Italy), has been tested in its two main horizontal directions, namely, Roll and Shear directions. The experimental campaign was aimed at investigating the dynamic and static behavior of the selected device in three different displacements ranges, that is, small, relatively large and large displacements ranges, under the effect of four different values of vertical load. Indeed, in the research literature, there are only experimental tests results obtained testing these metal devices within a relatively small displacements range [2], [6], [8].

The experimental investigation of the dynamic and static response of the tested HWRI has been performed by adopting a testing machine, available at the Laboratory of Department of Industrial Engineering of the University of Naples Federico II, which allows to impose both displacement or load histories in the horizontal direction, while the bearing is subjected to a constant vertical load.

The dynamic behavior of the tested device has been studied by analyzing the values of two parameters evaluated from the experimental hysteresis loops, that is, the average effective (or secant) stiffness and the average equivalent viscous damping ratio. The static tests have been performed to study the overall behavior of the devices, that is, to evaluate the values of static effective stiffness and of the static to dynamic effective stiffness ratio for different amplitudes and applied to vertical loads.

II. TESTED HELICAL WIRE ROPE ISOLATOR

HWRIs are metal devices consisting of a wire rope wound in the form of a helix and embedded into two drilled metal retainer bars. The rope is constructed by layering several strands around a central one.

The selected HWRI, manufactured by Powerflex S.r.l (Limatola, Italy), has a rope of six strands, each having 25 steel wires, plus a central one with 49 wires. The material of the cable is Stainless Steel Type 316, whereas the material of the two retainer bars is aluminum alloy.

Fig. 1 shows the geometrical characteristics of the tested HWRI and its two principal horizontal directions, namely, Roll and Shear directions.

N. Vaiana, PhD Student in Structural and Seismic Engineering, is with the Department of Structures for Engineering and Architecture, University of Napoli Federico II, via Claudio 21, 80125 Napoli, Italy (phone: 0039-329-1876763; e-mail: nicolovaiana@outlook.it).

M. Spizzuoco and G. Serino, Full Professor of Structural Engineering, are with the Department of Structures for Engineering and Architecture, University of Napoli Federico II, via Claudio 21, 80125 Napoli, Italy (e-mail: spizzuoc@unina.it, giorgio.serino@unina.it).
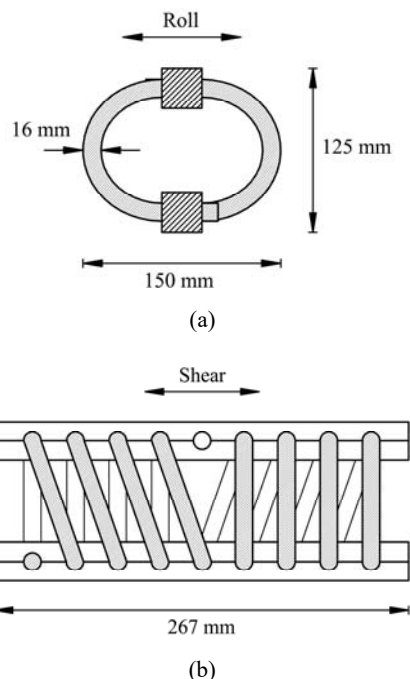
World Academy of Science, Engineering and Technology
International Journal of Civil and Environmental Engineering
Vol:11, No:2, 2017

(a)

(b)

Fig. 1 Geometrical characteristics and principal directions of the
tested HWRI: (a) Roll and (b) Shear directions

III. TESTING MACHINE

The experimental investigation of the dynamic and static behavior of the selected HWRI in the two principal horizontal directions has been performed by adopting a testing machine (Fig. 2) available at the Department of Industrial Engineering of the University of Naples Federico II (Italy).
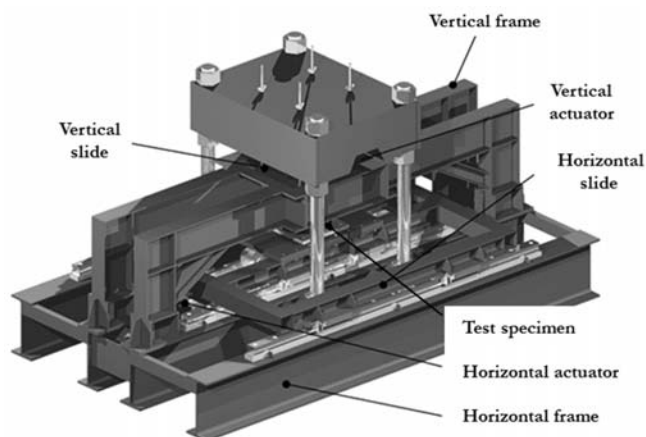

Fig. 2 Testing machine

The testing machine consists of a horizontal hydraulic actuator placed between a fixed base and a sliding table. The hydraulic actuator, powered by a 75 kW AC electric motor, allows to impose both displacement or load histories. The maximum horizontal force is 50 kN, the maximum speed is 2.2 m/s, the maximum stroke is ± 0.2 m. A hydraulic jack, positioned between the vertical reaction structure and the slide, allows to apply a vertical load up to 190 kN during the

tests [9].

The isolator under test is located between the sliding table and a slide that can move vertically with respect to the horizontal reaction structure. Figs. 3 (a) and (b) show the HWRI mounted in Roll and Shear directions, respectively, by fixing the aluminum retainer bars to the upper and lower rigid steel plates.
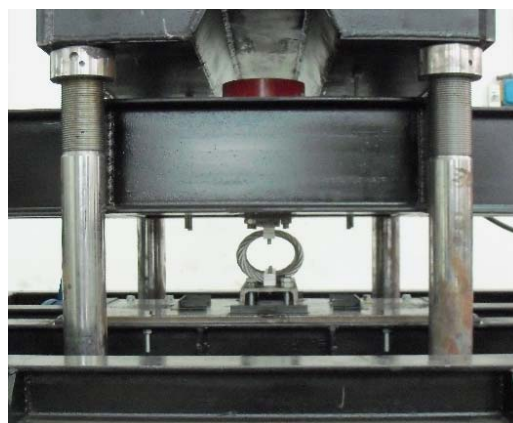
(a)
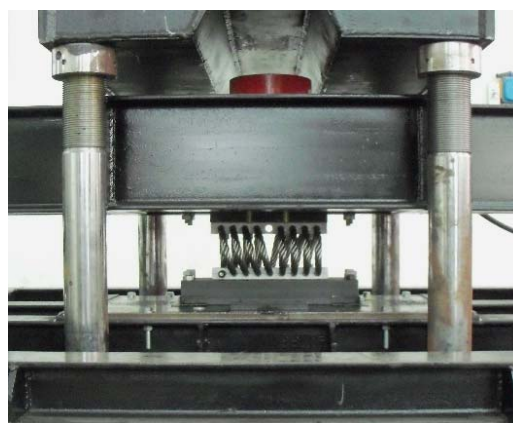
(b)

Fig. 3 HWRI mounted in: (a) Roll and (b) Shear directions

All tests were conducted by imposing horizontal displacements at room temperature and the data were sampled at 250 Hz. The relative horizontal displacement between the lower basement and the upper plate, the vertical load, and the lateral load time histories, has been measured.

IV. EXPERIMENTAL TESTS

Cyclic tests have been carried out in order to study the influence of displacement amplitude and vertical load on the dynamic behavior of the selected HWRI in both Roll and Shear directions.

Three different displacement amplitudes and four vertical load values have been chosen with the maximum value of the amplitude selected in order to avoid damages to the two aluminum alloy retainer bars during the experimental tests.

The testing procedure was as follows: Five fully reversed

World Academy of Science, Engineering and Technology
International Journal of Civil and Environmental Engineering
Vol:11, No:2, 2017

sinusoidal cycles of horizontal displacement, having specified amplitude A and frequency $f = 1$ Hz, were applied while the bearing was subjected to a constant vertical load P_v.

The dynamic displacement-controlled tests are listed in Table I.

TABLE I
DYNAMIC TESTS IN ROLL AND SHEAR DIRECTIONS

No. of Tests	Frequency [Hz]	Amplitude [cm]	Vertical Load [kN]
3+3	1	1, 3, 6	0
3+3	1	1, 3, 6	1.2
3+3	1	1, 3, 6	2
3+3	1	1, 3, 6	3

Static tests in Roll and Shear directions have been also conducted to study the overall behavior of the metal device, that is, to estimate the effective horizontal stiffness and to evaluate the static to dynamic effective stiffness ratio for different values of horizontal displacement and applied vertical load. In each static test, the horizontal displacement has been increased linearly with a velocity of 0.5 mm/s.

The static displacement-controlled tests are listed in Table II.

TABLE II
STATIC TESTS IN ROLL AND SHEAR DIRECTIONS

No. of Tests	Max. Displacement [cm]	Vertical Load [kN]
4+4	6	0, 1.2, 2, 3

V. EXPERIMENTAL TESTS RESULTS

In this section, the results of the dynamic and static experimental tests conducted on the selected HWRI are presented.

The parameters evaluated from the experimental force-displacement hysteresis loops to study the dynamic behavior of the tested device are the average effective (or secant) stiffness $k_{eff,a}$ and the average equivalent viscous damping ratio $\xi_{eq,a}$.

The effective stiffness, corresponding to each load cycle of a dynamic test, has been evaluated based on the peak lateral load and displacement as [10]:

$$k_{eff} = \frac{f_{max} - f_{min}}{u_{max} - u_{min}}, \qquad (1)$$

where f_{max}, f_{min}, u_{max}, and u_{min} are the peak values of horizontal load and displacement, respectively, at the extremes of the cyclic displacement range. The average effective stiffness $k_{eff,a}$ has been calculated as mean value of those obtained from three of the five experimental loading cycles.

The equivalent viscous damping ratio of the device at each cycle has been evaluated as [10]:

$$\xi_{eq} = \frac{E_d}{4\pi E_s}, \qquad (2)$$

where E_d represents the dissipated energy, that is, the area within the hysteresis loop, and E_s is the restored elastic energy expressed as:

$$E_s = \frac{1}{2} k_{eff} u_a^2, \qquad (3)$$

with u_a the average value of positive and negative maximum displacements. The average equivalent viscous damping ratio $\xi_{eq,a}$ has been calculated as mean value of those obtained from three of the five loading cycles applied to the device.

As far as the influence of the displacement amplitude on the dynamic behavior of the tested HWRI is concerned, Table III presents the values of the average effective stiffness and equivalent viscous damping ratio obtained for three different amplitudes without the effect of the vertical load.
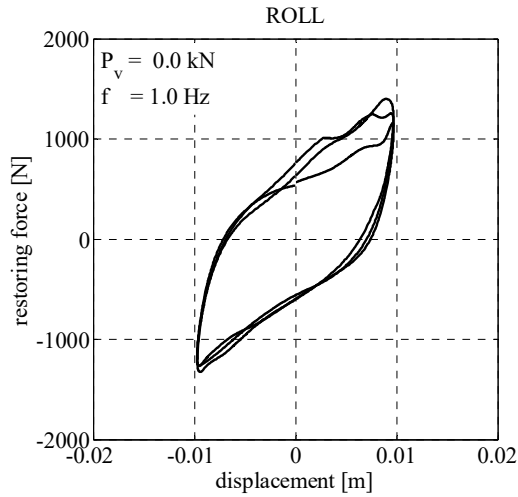
TABLE III
INFLUENCE OF DISPLACEMENT AMPLITUDE

$P_v = 0$ kN, $f = 1$ Hz	Amplitude [cm]	$k_{eff,a}$ [N/m]	$\xi_{eq,a}$ [%]
Roll	1	131616	26.9
	3	96411	14.7
	6	172987	8.0
Shear	1	157702	21.5
	3	125189	13.8
	6	178735	9.8

It can be observed that the tested metal device displays high effective stiffness and equivalent damping ratio at small displacements. These two parameters decrease with increasing displacement amplitude in the relatively large displacements range, whereas at larger displacements the former increases dramatically and the latter continues to decrease.
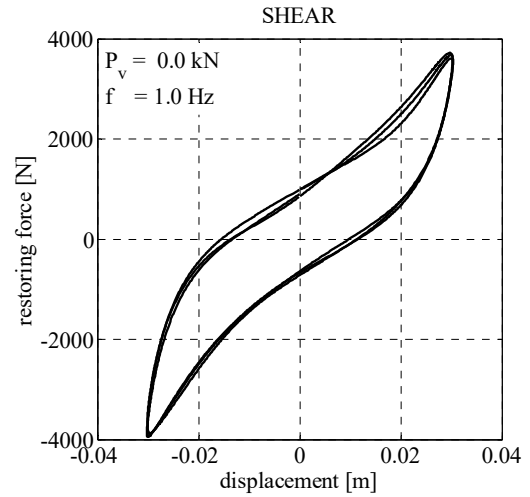
Figs. 4-6 show the symmetric force-displacement hysteresis loops obtained in Roll and Shear directions for the three different selected values of amplitude. It is worth to note that the shape of the hysteresis loops changes according to the displacements range: at small displacements the hysteresis loops display a softening stiffness (Fig. 4), whereas in the relatively large displacements range the device exhibits a hardening stiffness (Fig. 5). When large horizontal displacements are applied a stronger nonlinear stiffening behavior can be observed (Fig. 6).

As regards to the effect of the vertical load on the dynamic behavior of the tested metal device, Table IV shows the results obtained in the two horizontal principal directions for four different values of vertical load by applying a sinusoidal harmonic motion having amplitude equal to 3 cm and frequency of 1 Hz.

An examination of these results reveals that an increase in the vertical load produces a reduction in the average effective stiffness and a slight increase in the average equivalent viscous damping ratio. Thus, it can be observed that the application of a vertical load allows to have a more flexible device with higher equivalent viscous damping ratio.
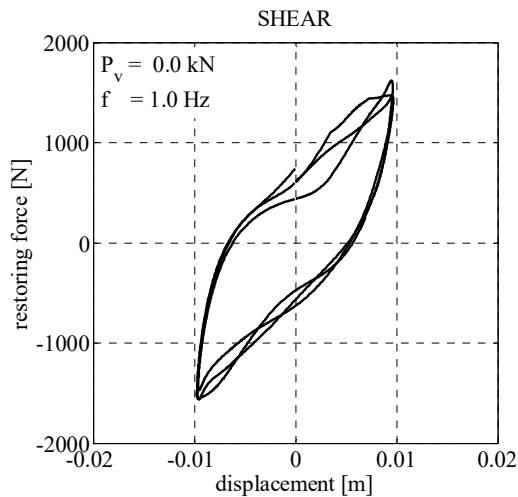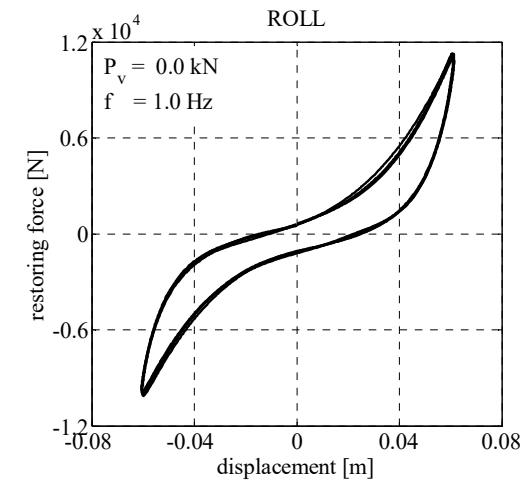
World Academy of Science, Engineering and Technology
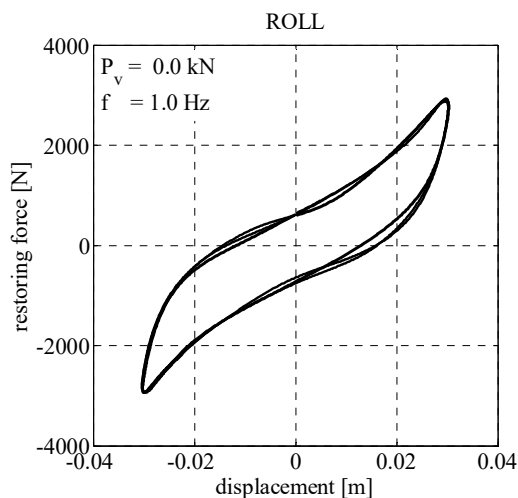International Journal of Civil and Environmental Engineering
Vol:11, No:2, 2017

(a)

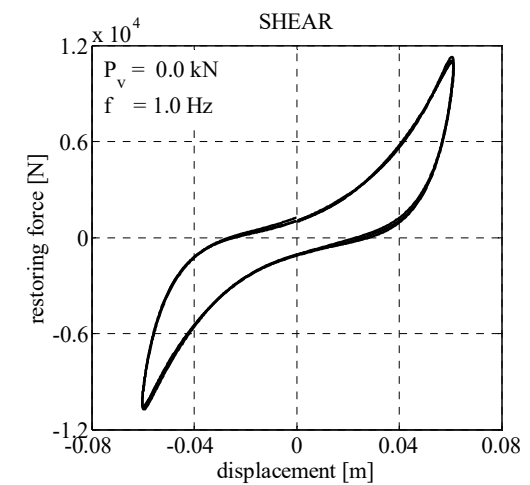(b)

Fig. 4 Hysteresis loop shape at small displacements in (a) Roll and (b) Shear directions

(a)

(b)

Fig. 5 Hysteresis loop shape at relatively large displacements in (a) Roll and (b) Shear directions

(a)

(b)

Fig. 6 Hysteresis loop shape at large displacements in (a) Roll and (b) Shear directions

World Academy of Science, Engineering and Technology
International Journal of Civil and Environmental Engineering
Vol:11, No:2, 2017

TABLE IV
INFLUENCE OF VERTICAL LOAD

$A = 3$ cm, $f = 1$ Hz	Vertical Load [kN]	$k_{eff,a}$ [N/m]	$\xi_{eq,a}$ [%]
Roll	0.0	96411	14.7
	1.2	84587	14.9
	2.0	73800	17.5
	3.0	63085	18.8
Shear	0.0	125189	13.8
	1.2	120047	12.3
	2.0	82622	14.5
	3.0	70673	15.7

The dynamic tests results obtained for $A = 1$ cm and $A = 6$ cm under the effect of the four different values of applied vertical load are omitted for brevity.

observed that at large displacements the applied vertical load affects much less the dynamic response of the metal device.

(a)

(b)

Fig. 8 Influence of vertical load at relatively large displacements in (a) Roll and (b) Shear directions
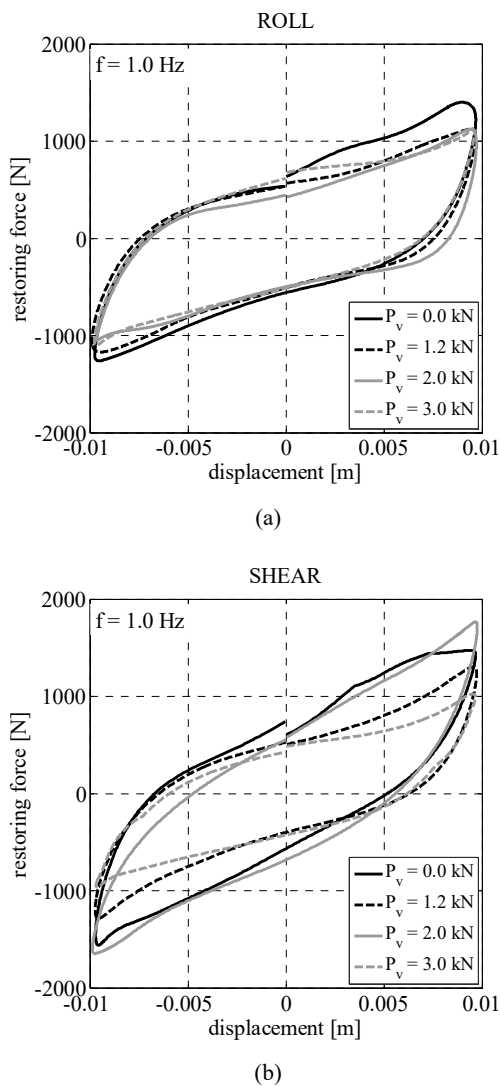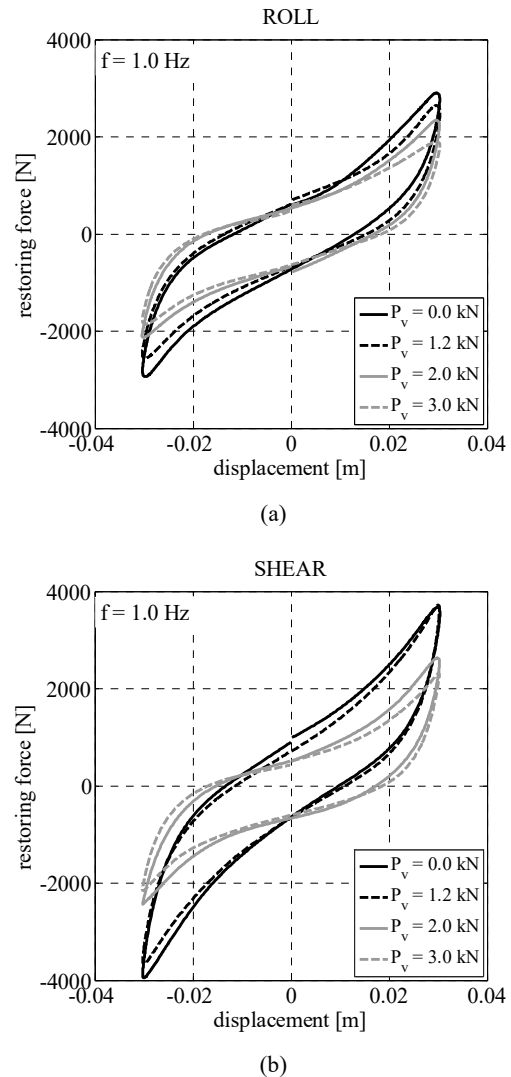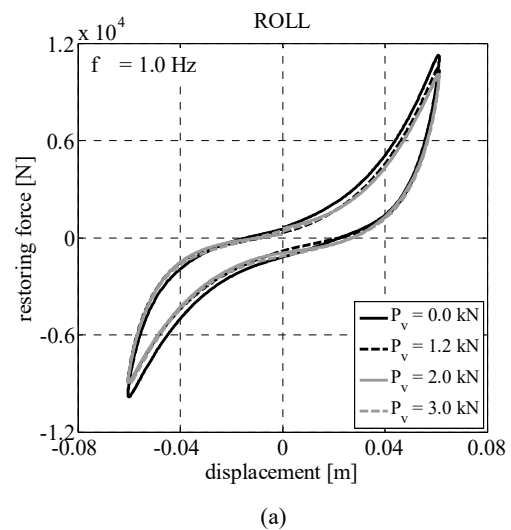

(a)

(a)

(b)

Fig. 7 Influence of vertical load at small displacements in (a) Roll and (b) Shear directions

Figs. 7-9 show the symmetric force-displacement hysteresis loops obtained in Roll and Shear directions under the effect of different values of vertical load at small (Fig. 7), relatively large (Fig. 8), and large displacements (Fig. 9). It can be

World Academy of Science, Engineering and Technology
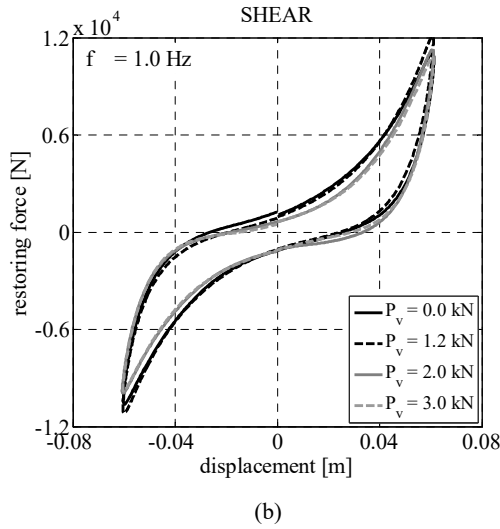International Journal of Civil and Environmental Engineering
Vol:11, No:2, 2017

(b)

Fig. 9 Influence of vertical load at large displacements in (a) Roll and (b) Shear directions

Static tests in both two horizontal directions were carried out by applying a horizontal displacement, increased linearly (v = 0.5 mm/s) up to a maximum value of 6 cm, under the effects of the four values of vertical load.

The static effective stiffness k_{eff}^{st} at displacement u^* has been estimated as:

$$k_{eff}^{st} = \frac{f(u^*)}{u^*}, \qquad (4)$$

where $f(u^*)$ is the recorded force corresponding to the applied displacement u^*.

Table V shows the values of static effective stiffness k_{eff}^{st} and of the static to dynamic effective stiffness ratio $k_{ratio} = k_{eff}^{st} / k_{eff}^{dyn}$ determined from experimental data. It can be observed that the latter parameter decreases with increasing displacement amplitude and tends to 1 for large displacement values.

TABLE V
STATIC TESTS RESULTS

$P_v = 0$ kN	Amplitude [cm]	k_{eff}^{st} [N/m]	k_{ratio}
Roll	1	223224	1.69
	3	142044	1.47
	6	174274	1.00
Shear	1	264560	1.67
	3	163781	1.30
	6	196837	1.10

Since the same static behavior has been observed testing the HWRI under the effect of different vertical loads, that is, 1.2, 2, and 3 kN, these results are omitted for brevity.

Fig. 10 (a) shows the force-displacement curves obtained for different vertical load values during the static tests in Roll

direction, whereas Fig. 10 (b) shows the deformed shape of the metal device displayed in Roll direction for an amplitude of 6 cm when no vertical load is applied.
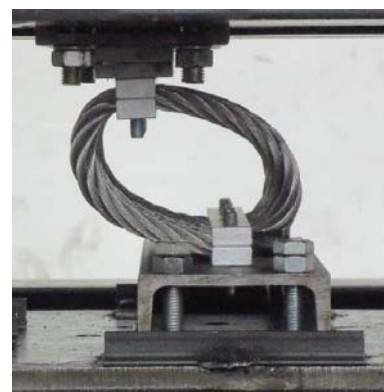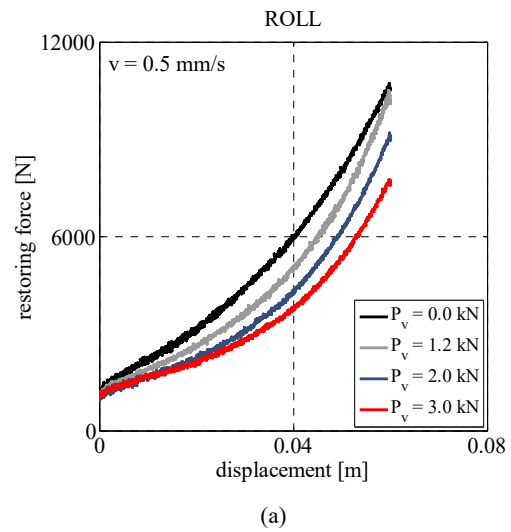

(a)

(b)

Fig. 10 Static tests in Roll direction: (a) force-displacement curves and (b) HWRI deformed shape for A = 6 cm and P_v = 0 kN

VI. CONCLUSIONS

The experimental investigation of the dynamic and static response of a HWRI, manufactured by Powerflex S.r.l (Limatola, Italy), has been performed by adopting a testing machine available at the Department of Industrial Engineering of the University of Naples Federico II which allows to impose horizontal displacement or load histories to the tested device with a constant vertical compression.

Each test consisted in imposing five cycles of sinusoidal displacement having specified amplitude and frequency, under four different values of vertical load. Three amplitude values have been chosen with the maximum one selected in order to avoid damages to the two aluminum alloy retainer bars of the device during the experimental tests. The loading frequency was assumed equal to 1 Hz.

According to experimental tests results, the tested device is characterized by high effective stiffness and equivalent damping ratio in the range of small displacements. These two

World Academy of Science, Engineering and Technology
International Journal of Civil and Environmental Engineering
Vol:11, No:2, 2017

parameters decrease with increasing displacement amplitude in the relatively large displacements range, whereas, at large displacements, the former increases dramatically and the latter continues to decrease. The shape of the hysteresis loops changes according to the displacements range: at small displacements, the hysteresis loops display a softening stiffness whereas, in the relatively large displacements range, the device exhibits a hardening stiffness. When large horizontal displacements occur, the metal device shows a stronger nonlinear stiffening behavior.

As far as the effect of the vertical load on the dynamic behavior of the tested HWRI is concerned, experimental results reveal a reduction in the effective stiffness and a slight increase in the equivalent viscous damping ratio due to the increase of the vertical load. Furthermore, it can be observed that, at large displacements, the applied vertical load affects much less the dynamic response of the metal device.

As regards the static tests results, the static to dynamic effective stiffness ratio decreases with increasing displacement amplitude and tends to 1 for large displacement values.

REFERENCES

[1] M. L. Tinker and M. A. Cutchins, "Damping phenomena in a wire rope vibration isolation system," *Journal of Sound and Vibration*, vol. 157, no. 1, pp. 7-18, 1992.
[2] G. F. Demetriades, M. C. Constantinou and A. M. Reinhorn, "Study of wire rope systems for seismic protection of equipment in buildings," *Engineering Structures*, vol. 15, no. 5, pp. 321-334, 1993.
[3] G. Serino, F. Bettinali and G. Bonacina, "Seismic base isolation of gas insulated electrical substations: comparison among different solutions," *Proceedings of the 4th US Conference on Lifeline Earthquake Engineering*, San Francisco, California, 1995.
[4] G. Serino, G. Bonacina and F. Bettinali, "Passive protection devices for high-voltage equipment: design procedures and performance evaluation," *Proceedings of the 4th US Conference on Lifeline Earthquake Engineering*, San Francisco, California, 1995.
[5] M. Di Donna and G. Serino, "Base isolation of high-voltage equipment: comparison between two different solutions," *Proceedings of the 7th International Conference on Probabilistic Methods Applied to Power Systems*, Napoli, Italy, 2002.
[6] S. Alessandri, R. Giannini, F. Paolacci and M. Malena, "Seismic retrofitting of an HV circuit breaker using base isolation with wire ropes. Part 1: Preliminary tests and analyses," *Engineering Structures*, vol. 98, pp. 251-262, 2015.
[7] G. De Canio, "Marble devices for the base isolation of the two bronzes of Riace: a proposal for the David of Michelangelo," *Proceedings of the 15th Word Conference on Earthquake Engineering*, Lisbon, Portugal, 2012.
[8] S. Alessandri, R. Giannini, F. Paolacci, M. Amoretti and A. Freddo, "Seismic retrofitting of an HV circuit breaker using base isolation with wire ropes. Part 2: Shaking-table test validation," *Engineering Structures*, vol. 98, pp. 263-274, 2015.
[9] S. Pagano, M. Russo, S. Strano and M. Terzo, "A mixed approach for the control of a testing equipment employed for earthquake isolation systems," *Journal of Mechanical Engineering Science*, vol. 228, no. 2, pp. 246-261, 2014.
[10] A. K. Chopra, *Dynamics of Structures: Theory and Applications to Earthquake Engineering*, 4th ed. Englewood Cliffs, NJ: Prentice Hall, 2012.